Non-nucleoside HIV-1 Reverse Transcriptase Inhibitors, Part 7.[1] Synthesis, Antiviral Activity, and 3D-QSAR Investigations of Novel 6-(1-Naphthoyl) HEPT Analogues

Lei JI,[a] Fen-Er CHEN,*,[a] Xiao-Qing FENG,[a] Erik De CLERCQ,[b] Jan BALZARINI,[b] and Christophe PANNECOUQUE[b]

[a] *Department of Chemistry, Fudan University; Shanghai 200433, People's Republic of China: and* [b] *Rega Institute for Medical Research, Katholieke Universiteit Leuven; 10 Minderbroedersstraat, B-3000 Leuven, Belgium.*

Received February 13, 2006; accepted April 26, 2006

A series of novel 1-[(2-hydroxyethoxy)methyl]-6-(phenylthio)thymine (HEPT) analogues bearing a 6-(1-naphthoyl) group of non-nucleoside human immunodeficiency virus (HIV) reverse transcriptase inhibitors were synthesized and evaluated for their activity against HIV-1 and HIV-2. It was found that most of these compounds showed good activity against HIV-1. Among them, compound 5-isopropyl-6-(1-naphthoyl)-1-[(2*E*)-3-phenylallyl]-2,4-pyrimidinedione (23) displayed the greatest inhibitory potency (IC_{50}=0.14 μM), which is about 35-fold more active than HEPT and DDI. To rationalize the relationships between structure and activity of these novel compounds, a three-dimensional quantitative structure–activity relationship (3D-QSAR) model was also generated. The results provided a tool for guiding the further design of more potent antiviral agents and for predicting the affinity of related compounds.

Key words HIV-1 reverse transcriptase inhibitor; antiviral activity; synthesis; 3D-QSAR; 6-(1-naphthoyl)

Non-nucleoside reverse transcriptase inhibitors (NNRTIs)[2] play an essential role in the therapy for AIDS due to their potent antiviral activity, high specificity, and low toxicity. Among the representatives of the NNRTIs, 1-[(2-hydroxyethoxy)methyl]-6-(phenylthio)thymine (**1**, HEPT),[3—5] has an interesting structure and highly anti-HIV-1 specific activity that has induced many kinds of structural modifications on the skeleton of thymine as a lead compound (Fig. 1). It was found that an aromatic ring structure at the C-6 of the thymine moiety is an important determinant for the anti-HIV activity.[6]

In previous papers, we have reported the synthesis of a series of 6-naphthylmethyl and 6-naphthylthio substituted HEPT analogues (HEPTs), and found that most of them exhibited highly potent anti-HIV-1 activity. For example, 1-benzoxymethyl-5-isopropyl-6-(1-naphthylmethyl)uracil (**2**)[7] and 1-ethoxymethyl-5-isopropyl-6-(1-naphthylthio)uracil (**3**)[8] showed highly potent anti-HIV-1 activity with IC_{50} of 17 and 57 nM, respectively (Fig. 1). Based on our previous research in this field, we postulate that the introduction of a 6-(1-naphthoyl) group as a H-bond acceptor to the C-6 position of HEPTs may be more beneficial to enhance the interaction between the inhibitors and reverse transcriptase (RT).[9] With the aim to examine our assumption and find more potent new anti-HIV agents, in this paper we describe the synthesis and antiviral activity of a series of novel 6-(1-naphthoyl) substituted HEPTs (**4**, Fig. 1).

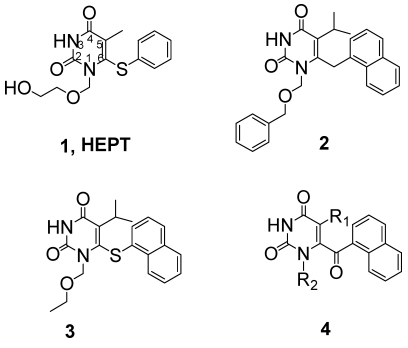

Fig. 1

Chemistry

The target compounds in this study were synthesized as shown in Chart 1. The barbituric acid derivatives **6a**, **b** were known to be readily available from urea and diethyl malonic esters **5a**, **b**. The barbituric acid derivatives **6a**, **b** were converted to the corresponding trichloropyrimidines **7a**, **b** by reaction of $POCl_3$ and dimethylaniline under reflux for 2 h in 80—85% yields.[10]

Treatment of **7a**, **b** with NaOMe in MeOH at −3 °C for

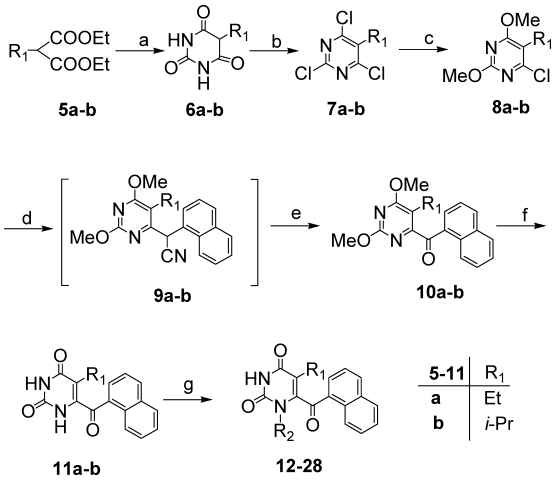

Reagents and conditions: (a) urea, MeONa, MeOH, reflux 10 h, 75—80%; (b) $POCl_3$, dimethylaniline, 80—85%; (c) MeONa, MeOH, 72—78%; (d) 1-naphthylacetonitrile, 60% NaH, DMF, N_2; (e) 60% NaH, DMF, air, 80—90% (one-pot synthesis); (f) conc. HCl, MeOH, reflux 24—48 h; (g) R_2X (X=Br, Cl), K_2CO_3, DMF, rt 24—36 h, 35—60%.

Chart 1. Synthesis of the Target Compounds (**12**—**28**)

* To whom correspondence should be addressed. e-mail: rfchen@fudan.edu.cn

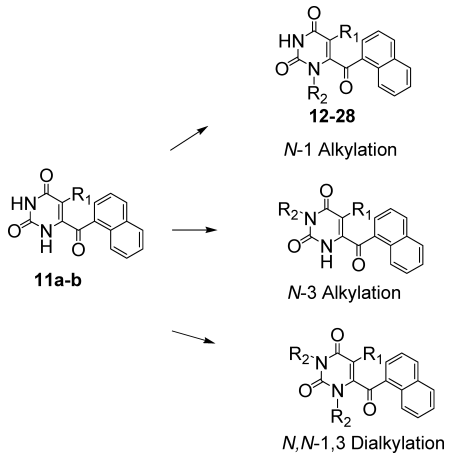

Chart 2

24—36 h led to the corresponding 5-alkyl-6-chloro-2,4-dimethoxypyrimidines **8a**, **b**.[11] Condensation of **8a**, **b** with 1-naphthylacetonitrile in the presence of 60% NaH in anhydrous DMF for 48 h at room temperature under N_2 gave the corresponding nitriles **9a**, **b**, which, without separation, were immediately oxidized to the ketones **10a**, **b** by passing air into the reaction mixture at room temperature. Demethylation of **10a**, **b** with conc. HCl in refluxing MeOH for 24—48 h afforded the 5-alkyl-6-(1-naphthoyl)-2,4-pyrimidinediones **11a**, **b**, which were subjected to *N*-1 alkylation with various halids in the presence of anhydrous K_2CO_3 in anhydrous DMF to afford the desirable target compounds **12**—**28**. It is worth mentioning that in this *N*-1 alkylation reaction, some by-products such as *N*-3 alkylation and *N*,*N*-1,3 dialkylation compounds (Chart 2) were also formed, just as we have described previously.[7] The *N*-1 alkylation compounds **12**—**28** were the main products, which could be purified by column chromatography (eluent: ethyl acetate : hexane).

All the target compounds **12**—**28** were characterized by NMR, MS, and elemental analysis. Both analytical and spectral data of all the compounds are in full agreement with the proposed structures.

The structure determination of the target compounds of *N*-1 alkylation relies heavily on the application of protondetected heteronuclear NMR experiments. Perhaps the most useful of these methods is the two-dimensional ^1H–^{13}C heteronuclear multiple-bond correlation (HMBC) experiment, which provides correlations between protons and carbons over two and three bonds. Thus the *N*-1 substitutent compound was further confirmed by HMBC. No *N*-3 regioisomer was detected.

Results and Discussion

All the synthesized compounds were evaluated for anti-HIV activity and cytotoxicity against wild type HIV-1 strain III_B and HIV-2 ROD in MT-4 cells using the MTT method.[12] The inhibitory concentration of compounds was expressed as the concentration that caused 50% inhibition of viral cytopathogenicity (IC_{50}) without direct toxicity to the cells. The cytotoxic concentration (CC_{50}) of the compounds was monitored based on the growth of noninfected cells by the trypan blue exclusion method and corresponded to the concentration required to cause 50% cell death. Results were compared with the antiviral activity of HEPT and 2,3-dideoxyinosine (DDI). All results, expressed as IC_{50}, CC_{50}, and SI, are summarized in Table 1.

As seen from the results listed in Table 1, most of the tested compounds showed good activity against wild-type HIV-1 with a wide range of IC_{50} values from 6.60 to 0.14 μM, except for compounds **17** and **24**. Among them, 5-isopropyl-6-(1-naphthoyl)-1-[(2*E*)-3-phenylallyl]-2,4-pyrimidinedione (**23**) was the most promising compound and could be used to summarize as the favorable molecular features for interaction with RT. It displayed the greatest inhibitory potency activity against HIV-1 replication with an IC_{50} value of 0.14 μM, which is about 35 times more potent than HEPT and DDI, and a CC_{50} value of 21.23 μM. The viral selectivity index was 153, which is much better than those found from HEPT and DDI. Compounds (**15**, **22**) also showed good anti-HIV-1 potency (IC_{50}=0.19 and 0.17 μM, respectively) and good selectivity indices (SI=144 and 206, respectively).

Thus it can be seen that some *N*-1 side chains are suitable to improve the anti-HIV-1 activity, such as allyl, (2*E*)-3-phenylallyl, methoxycarbonylallyl, and benzyl. The factors responsible for the improved inhibitory potency of these compounds remain to be elucidated. One explanation may be that these *N*-1 substituent groups have suitable length to make interactions with the RT. On the other hand, these groups could interact with RT-amino acid Phe227 or Pro236 through π-stacking. The (2*E*)-3-phenylallyl group was the best, which could be due to its steric interactions with the adjacent amino acids. This is also confirmed by the CoMFA analysis. However, introduction of some groups at the *N*-1 site resulted in lower activity and higher cytotoxicity, *e.g.,* 4-methoxybenzoylmethyl, solanesyl, and 2-propynyl. This might be ascribed to their unsuitable length or unsuitable configuration to make interaction with RT-amino acid Phe227 or Pro236.

Interestingly, in the *N*-1 alkylation for preparation of the target compound **23**, one *N*,*N*-1,3 dialkylation by-product 1,3-di[(2*E*)-3-phenylallyl]-5-isopropyl-6-(1-naphthoyl)-2,4-pyrimidinedione (**29**) was also isolated and evaluated against HIV-1 and HIV-2. Compared with compound **23**, compound **29** exhibited less activity and much higher cytotoxicity (IC_{50}>129.39 μM and SI<1). It has been deduced that the 3-NH function enhances anti-HIV activity by donation of a hydrogen bond to the carbonyl oxygen of Lys101 in RT.[13] Therefore our results further confirm that the 3-NH function is essential for inhibition of HIV RT to HEPT analogues.

The triggering effect of 5-alkyl on interaction with the active binding site was the same as shown in the previous relative QSAR study.[14,15] It showed that inhibitory activity increased proportionally to the modification of the C-5 substituent in the order Et→*i*-Pr, where the influence of the isopropyl substituent is much greater than that of the ethyl substituent. Besides the anti-HIV-1 activity, we also evaluated activity against HIV-2 ROD, and found that all of the compounds showed less activity against HIV-2 in comparision with that against HIV-1.

3D-QSAR Analysis With the aim to rationalize the relationships between structure and activity of these novel compounds, we also conducted 3D-QSAR analyses. We applied 3D-QSAR methods, comparative molecular field analysis (CoMFA) to training our compounds **12—17**, **19**—**27** and

Table 1. Anti-HIV Activity in MT-4 Cells of Compounds **12**—**29**

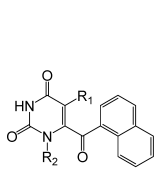

12-28

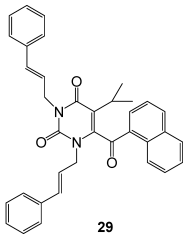

29

Compd.	R_1	R_2	IC_{50} (μM)[a]		CC_{50} (μM)[b]	SI[c]
			HIV-1 III_B	HIV-2 ROD		
12	Et	CH_2=$CHCH_2$	0.60±0.09	>39.22	39.22±5.12	64
13	Et	$(CH_3)_2C$=$CHCH_2$	6.60±2.46	>36.33	36.33±6.10	6
14	Et	$H_3COOCCH$=$CHCH_2$	0.92±0.00	>34.44	34.44±7.19	37
15	Et	*trans*-PhCH=$CHCH_2$	0.19±0.05	>28.71	28.71±12.97	144
16	Et	$PhCH_2$	1.07±0.18	>33.67	33.67±4.37	32
17	Et	(4′-OCH_3)$PhCOCH_2$	>28.75	>28.75	28.75±6.70	<1
18	Et	CH_3OOCCH_2	1.12±0.08	>167.62	167.62±39.34	148
19	Et	HC≡CCH_2	>4.82	>4.82	4.82±2.68	<1
20	Et	$MeOCH_2$	5.89±0.56	>34.35	34.35±4.17	6
21	Et	$MeOCH_2CH_2OCH_2$	5.71±1.28	>164.27	164.27±40.18	29
22	*i*-Pr	CH_2=$CHCH_2$	0.17±0.06	>37.10	37.10±7.24	206
23	*i*-Pr	*trans*-PhCH=$CHCH_2$	0.14±0.02	>21.23	21.23±10.97	153
24	*i*-Pr	*trans*-[CH_2CH=$C(CH_3)CH_2]_9H$	>72.01	>72.01	72.01±19.41	<1
25	*i*-Pr	$PhCH_2$	0.30±0.00	>33.54	33.54±3.04	111
26	*i*-Pr	$EtOOCCH_2$	1.42±0.51	>37.01	37.01±6.85	26
27	*i*-Pr	HC≡CCH_2	≥1.21	>4.10	4.10±2.77	≤3
28	*i*-Pr	$MeOCH_2$	0.88±0.26	>42.98	42.98±9.03	48
29			>129.39	>129.39	≥129.39	<1
HEPT			5.06	>405.8	405	80
DDI			5.37	2.71	≥529	≥98

a) Concentration required to protect the cell against viral cytopathogenicity by 50% in MT-4 cells. *b*) Concentration that reduces the normal uninfected MT-4 cell viability by 50%. *c*) Selectivity index: ratio CC_{50}/IC_{50}, a higher SI means a more selective compound.

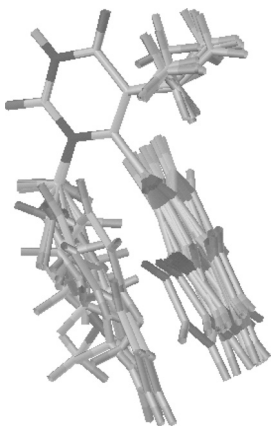

Fig. 2. 3D-View of All Aligned Compounds

29. Compounds **18** and **28** were used as the test set. The aligned molecules are shown in Fig. 2.

Partial least squares (PLS), the statistical method used in deriving 3D-QSAR models, is an extension of multiple regression analysis in which the original variables are replaced by a small set of their linear combinations.[16—18] Leave-one-out (LOO) cross-validated PLS analyses were used to check the predictive ability of the models and to determine the optimal number of components to be used in the final QSAR models. With all the compounds' inhibitory activity as response variable, initial CoMFA PLS analyses of the 16 compounds gave low cross-validated coefficients (q^2) values. Removal of outliers, compounds **17**, **24**, and **29**, based on residual values afforded models with q^2 value of 0.646, with the number of partial least squares (PLS) components of 4. The regression coefficients (r^2) value was up to 0.975. The results from the CoMFA studies are summarized in Table 2. The

Table 2. Summary of CoMFA Model

Model	q^2	N	r^2	S.E.	F	Static	Elec
CoMFA	0.646	4	0.975	0.118	78.634	0.672	0.328

Table 3. Experimental Activities and Predictive Activities by CoMFA of the Training Set

Compd.	pIC_{50}	CoMFA	Error
12	6.22	6.26	−0.04
13	5.18	5.04	0.14
14	6.04	6.04	0.00
15	6.72	6.69	0.03
16	5.97	6.00	−0.03
19	5.32	5.43	−0.11
20	5.23	5.17	0.06
21	5.24	5.29	−0.05
22	6.77	6.59	0.18
23	6.85	6.94	−0.09
25	6.52	6.42	0.10
26	5.85	5.96	−0.11
27	5.92	6.00	−0.08

quality of the final CoMFA method is measured by two statistical parameters: r^2 and q^2. The value of r^2 shows the self-consistency of the model and should be greater than 0.90. The value of q^2, which exhibits the predictive capacity of the model, should be greater than 0.40. These results indicate stability of our CoMFA model. The predictive ability of the model was further validated using two compounds (**18**, **28**) on account of the number of our compounds is limited. The experimental activities and the predicted activities using our CoMFA model and the residue values of the training set and the test set are given in Tables 3 and 4, respectively. A graph of the actual pIC_{50} *vs.* the predicted pIC_{50} values for the training set compounds by the CoMFA models based on com-

Table 4. Experimental Activities and Predictive Activities by CoMFA of the Test Set

Compd.	pIC_{50}	CoMFA	Error
18	5.95	5.56	0.39
28	6.06	6.09	−0.03

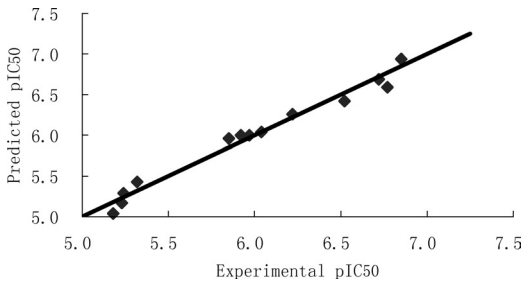

Fig. 3. Predictive *vs.* Experimental pIC_{50} Values Derived from the CoMFA Model of the Training Set

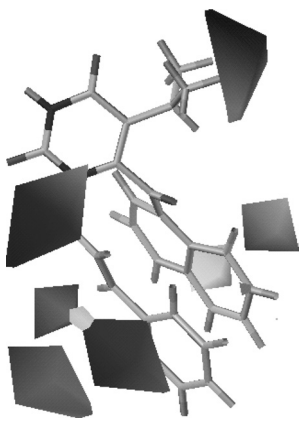

Fig. 4. CoMFA Contour Map

Green contours indicate regions where a bulky substituent increases potency, red contours show areas where electronegative substituent increases potency.

Table 6. Physical Data of the Target Compounds

Compd.	Formula	Analysis (%), Calcd (Found)		
		C	H	N
12	$C_{20}H_{18}N_2O_3$	71.84 (72.05)	5.43 (5.44)	8.38 (8.35)
13	$C_{22}H_{22}N_2O_3$	72.91 (72.80)	6.12 (6.13)	7.73 (7.71)
14	$C_{22}H_{20}N_2O_5$	67.34 (67.46)	5.14 (5.13)	7.14 (7.15)
15	$C_{26}H_{22}N_2O_3$	76.08 (76.34)	5.40 (5.38)	6.82 (6.81)
16	$C_{24}H_{20}N_2O_3$	74.98 (74.83)	5.24 (5.25)	7.29 (7.27)
17	$C_{26}H_{22}N_2O_5$	70.58 (70.81)	5.01 (5.02)	6.33 (6.31)
18	$C_{20}H_{18}N_2O_5$	65.57 (65.65)	4.95 (4.96)	7.65 (7.68)
19	$C_{20}H_{16}N_2O_3$	72.28 (72.03)	4.85 (4.84)	8.43 (8.46)
20	$C_{19}H_{18}N_2O_4$	67.44 (67.60)	5.36 (5.38)	8.28 (8.25)
21	$C_{21}H_{22}N_2O_5$	65.96 (66.05)	5.80 (5.82)	7.33 (7.34)
22	$C_{21}H_{20}N_2O_3$	72.40 (72.14)	5.79 (5.78)	8.04 (8.07)
23	$C_{27}H_{24}N_2O_3$	76.39 (76.68)	5.70 (5.72)	6.60 (6.62)
25	$C_{25}H_{22}N_2O_3$	75.36 (75.19)	5.57 (5.58)	7.03 (7.02)
26	$C_{22}H_{22}N_2O_5$	66.99 (67.23)	5.62 (5.60)	7.10 (7.12)
27	$C_{21}H_{18}N_2O_3$	72.82 (72.64)	5.24 (5.25)	8.09 (8.06)
28	$C_{20}H_{20}N_2O_4$	68.17 (68.39)	5.72 (5.74)	7.95 (7.98)

Table 5. Physical Data of the Target Compounds

Compd.	Yield (%)	Property	mp (°C)	ESI-MS (*m/z*, $[M+H]^+$)
12	57.3	A light yellowish powder	189.3—190.5	335
13	36.5	A yellow powder	130.0—131.2	363
14	35.0	An orange powder	108.1—109.3	393
15	59.3	Light yellowish crystals	101.6—102.7	411
16	50.7	A white powder	221.2—222.8	385
17	22.9	A yellow powder	232.1—233.2	443
18	37.5	A yellow powder	186.1—187.2	367
19	38.5	A white powder	191.3—191.5	333
20	57.2	A light yellowish powder	131.0—132.4	339
21	55.1	A white powder	118.0—119.1	383
22	49.2	A white powder	196.0—196.2	349
23	60.1	White crystals	130.8—131.9	425
25	50.9	A white powder	224.4—225.3	399
26	50.6	A white powder	169.1—169.6	395
27	57.2	A white powder	192.3—193.6	347
28	59.1	A white powder	173.1—174.4	353

pound **23** is shown in Fig. 3.

The CoMFA coefficient contour maps for the inhibitory activity are shown in Fig. 4. A green contour near the 5-position of the HEPT analogues indicates that bulky substituents at this position increase activity. This conclusion is consistent with the results of our experiments showing that 5-ethyl substituted compounds (**12**—**21**) are generally less active than 5-isopropyl substituted compounds (**22**—**28**). A blue contour around the 1-methylene attached to the 2,4-pyrimidinedione ring suggests that electronegative groups at this location might decrease potency. Both the yellow and the red contours appearing near the end of the allyl moiety suggest that a small and electronegative substituent at this position will enhance inhibitory potency. Compounds **15** and **23** with an electronegative group, (2*E*)-3-phenylallyl, exhibit higher activity. A comparison of compounds **13** and **14** shows that a change from two methyl to one methoxycarbonyl group at the end of the allyl group increases the potency, which may be due to an decrease in the steric bulk of the group. This also can be seen from compounds **12** and **13**.

Conclusion

In summary, we have described the synthesis and anti-HIV activity of novel 6-(1-naphthoyl) substituted HEPT analogues. The results showed that most of these analogues exhibited moderate or high activity against HIV-1. The most active compound **23** exhibited about 35-fold more active anti-HIV-1 activity than HEPT and DDI. These results confirmed our assumption that the introduction of a 1-naphthoyl substituent to the C-6 position of HEPTs might improve the antiviral activity since it was more favorable to enhance the interaction between the inhibitors and RT. We also have done a detailed 3D-QSAR study for better understanding their inhibitory properties. These results provide a tool for guiding further drug design and for predicting the affinity of related compounds. As a result, our studies provide useful indicators for guiding the further rational design of more potent new HEPT analogues.

Experimental

Melting points were measured on a WRS-1 digital melting point instrument and are uncorrected. ^{1}H-, ^{13}C-NMR, and HMBC spectra were recorded in dimethylsulfoxide-d_6 (DMSO-d_6) or chloroform ($CDCl_3$) on a Brucker DMX 500 MHz spectrometer. Chemical shifts are reported in δ (ppm) units

Table 7. Physical Data of the Target Compounds

Compd.	NMR δ (DMSO-d_6 or $CDCl_3$)
12	^{1}H-NMR (DMSO-d_6) δ: 0.82 (3H, t, J=7.3 Hz), 1.99—2.08 (2H, m), 3.94—4.28 (2H, m), 4.85—4.98 (2H, m), 5.62—5.70 (1H, m), 7.66—9.13 (7H, m), 11.67 (1H, s). ^{13}C-NMR (DMSO-d_6) δ: 13.82, 18.31, 47.01, 116.56, 118.03, 124.89—137.12 (11C), 145.86, 150.97, 163.49, 191.45.
13	^{1}H-NMR (DMSO-d_6) δ: 0.80 (3H, t, J=7.3 Hz), 1.05 (3H, s), 1.32 (3H, s), 1.94—2.06 (2H, m), 4.12—4.17 (2H, m), 4.96 (1H, m), 7.66—9.18 (7H, m), 11.62 (1H, s). ^{13}C-NMR (DMSO-d_6) δ: 12.84, 17.45, 20.78, 25.98, 39.78, 114.65, 115.02, 125.36—137.72 (11C), 145.17, 150.97, 163.59, 191.20.
14	^{1}H-NMR (DMSO-d_6) δ: 0.81 (3H, t, J=7.2 Hz), 1.99—2.16 (2H, m), 3.60 (3H, s), 4.04—4.18 (2H, m), 5.68 (1H, d, J=15.9 Hz), 6.61—6.66 (1H, m), 7.63—9.11 (7H, m), 11.70 (1H, s). ^{13}C-NMR (DMSO-d_6) δ: 13.59, 18.67, 39.85, 53.48, 116.82, 123.59—137.42 (11C), 142.76, 145.34, 150.68, 163.93, 167.01, 191.47.
15	^{1}H-NMR ($CDCl_3$) δ: 0.98 (3H, t, J=7.3 Hz), 2.16—2.31 (2H, m), 4.42 (2H, d, J=6.1 Hz), 6.02—6.05 (1H, m), 6.10 (1H, d, J=15.9 Hz), 7.02—7.20 (5H, m), 7.45—8.61 (7H, m), 9.34 (1H, s). ^{13}C-NMR (DMSO-d_6) δ: 11.78, 15.49, 46.17, 118.86, 125.68—137.29 (17C), 145.06, 150.48, 163.75, 191.50.
16	^{1}H-NMR (DMSO-d_6) δ: 0.80 (3H, t, J=7.2 Hz), 1.80—2.10 (2H, m), 4.65—4.87 (2H, m), 7.04—7.18 (5H, m), 7.52—9.04 (7H, m), 11.76 (1H, s,). ^{13}C-NMR (DMSO-d_6) δ: 12.59, 18.58, 47.68, 117.57, 122.33—141.95 (15C), 146.13, 151.05, 163.97, 191.32.
17	^{1}H-NMR (DMSO-d_6) δ: 0.79 (3H, t, J=7.3 Hz), 1.99—2.02 (2H, m), 3.78 (3H, s), 5.05 (2H, m), 6.91—8.94 (11H, m), 11.79 (s, 1H, NH). ^{13}C-NMR (DMSO-d_6) δ: 13.00, 19.08, 55.87, 56.11, 119.98—135.98 (15C), 145.93, 151.03, 163.86, 165.20, 191.29, 195.69.
18	^{1}H-NMR (DMSO-d_6) δ: 0.77 (3H, t, J=7.3 Hz), 1.99 (2H, m), 3.53 (3H, s), 4.20—4.41 (2H, m), 7.67—9.06 (7H, m), 11.85 (1H, s). ^{13}C-NMR (DMSO-d_6) δ: 13.04, 18.98, 45.53, 51.52, 115.67, 124.17—136.94 (10C), 145.73, 151.13, 163.68, 169.71, 191.42.
19	^{1}H-NMR ($CDCl_3$-d_6) δ: 0.94 (3H, t, J=7.4 Hz), 2.17 (1H, s), 2.25 (2H, m), 4.31—4.60 (2H, m), 7.55—8.53 (7H, m), 9.27 (1H, s). ^{13}C-NMR (DMSO-d_6) δ: 13.64, 19.03, 32.01, 70.87, 78.37, 115.92, 125.49—137.01 (10C), 143.65, 151.01, 163.73, 191.44.
20	^{1}H-NMR (DMSO-d_6) δ: 0.79 (3H, t, J=7.3 Hz), 1.99 (2H, m), 3.09 (3H, s), 5.00 (2H, s), 7.65—9.08 (7H, m), 11.72 (1H, s). ^{13}C-NMR (DMSO-d_6) δ: 12.92, 19.01, 56.52, 77.11, 114.93, 125.17—136.98 (10C), 146.75, 151.06, 163.23, 191.35.
21	^{1}H-NMR (DMSO-d_6) δ: 0.78 (3H, t, J=7.2 Hz), 1.99 (2H, m), 3.02 (3H, s), 3.11—3.73 (4H, m), 5.10—5.36 (2H, m), 7.70—9.10 (7H, m), 11.70 (1H, s). ^{13}C-NMR (DMSO-d_6) δ: 12.87, 18.7, 59.56, 67.54, 73.01, 75.33), 115.03, 126.97—137.00 (10C), 146.86, 151.14, 163.34, 191.39.
22	^{1}H-NMR (DMSO-d_6) δ: 1.14 (6H, d, J=6.8 Hz), 2.30 (1H, sep, J=6.8 Hz), 3.90 (1H, d, J=14.9 Hz), 4.26 (1H, d, J=14.6 Hz), 4.84—4.97 (2H, m), 5.61—5.68 (1H, m), 7.68—9.20 (7H, m), 11.55 (1H, s). ^{13}C-NMR (DMSO-d_6) δ: 21.01, 24.79, 45.91, 117.31, 120.25, 126.97—135.27 (11C), 142.55, 151.00, 163.79, 191.45.
23	^{1}H-NMR ($CDCl_3$) δ: 1.18 (6H, d, J=6.9 Hz), 2.50 (1H, sep, J=6.9 Hz), 4.37—4.41 (2H, m), 6.00—6.02 (1H, m), 6.07 (1H, d, J=15.9 Hz), 7.00—7.19 (5H, m), 7.46—8.10 (7H, m), 9.41 (1H, s). ^{13}C-NMR (DMSO-d_6) δ: 20.98, 24.23, 45.69, 119.92, 126.11—135.91 (17C), 142.05, 151.56, 163.58, 191.37.
25	^{1}H-NMR (DMSO-d_6) δ: 1.16 (6H, d, J=6.8 Hz), 2.29 (1H, sep, J=6.8 Hz), 4.61 (1H, d, J=15.5 Hz), 4.85 (1H, d, J=15.5 Hz), 7.02—7.16 (5H, m), 7.54—9.12 (7H, m), 11.64 (1H, s). ^{13}C-NMR (DMSO-d_6) δ: 20.65, 24.97, 47.96, 119.68, 126.79—136.76 (14C), 141.32, 141.97, 150.98, 163.88, 191.35.
26	^{1}H-NMR (DMSO-d_6) δ: 1.11 (6H, d, J=6.9 Hz), 1.15 (3H, t, J=7.0 Hz), 2.30 (1H, sep, J=6.9 Hz), 3.94 (2H, m), 4.13—4.37 (2H, m), 7.69—9.14 (7H, m), 11.73 (1H, s). ^{13}C-NMR (DMSO-d_6) δ: 14.32, 21.78 (d), 28.76, 46.94 (NCH_2), 119.63, 127.37—136.46 (10C), 141.32, 150.45, 163.90, 170.03, 191.77.
27	^{1}H-NMR (DMSO-d_6) δ: 1.14 (6H, d, J=6.8 Hz), 2.31 (1H, sep, J=6.8 Hz), 3.14 (1H, s), 4.22—4.34 (2H, m), 7.69—9.23 (7H, m), 11.66 (1H, s). ^{13}C-NMR (DMSO-d_6) δ: 21.64 (d), 28.03, 32.01, 70.87, 78.37, 119.92, 125.49—137.01 (10C), 142.65, 151.61, 163.73, 191.44.
28	^{1}H-NMR (DMSO-d_6): δ: 1.13 (6H, d, J=6.8 Hz), 2.31 (1H, sep, J=6.8 Hz), 3.07 (3H, s), 4.96—5.04 (2H, m), 7.68—9.18 (7H, m), 11.61 (1H, s). ^{13}C-NMR (DMSO-d_6) δ: 22.00 (d), 27.13, 56.51, 77.90, 119.42, 127.07—135.79 (10C), 141.55, 150.27, 163.36, 191.40

relative to the internal standard tetramethylsilane (TMS). Mass spectra were obtained on a MAT-95 mass spectrometer. Elemental analyses were performed on a CARLOERBA 1106 instrument and the results of elemental analyses for C, H, and N were within ±0.4% of the theoretical values. All chemicals and solvents used were of reagent grade and were purified and dried by standard methods before use. All air-sensitive reactions were run under a nitrogen atmosphere. All reactions were monitored by TLC on precoated silica gel G plates at 254 nm under a UV lamp using ethyl acetate/hexane as eluents. Silica column chromatography separations were obtained on silica gel (300—400 mesh).

Biological Activity Assays The anti-HIV activity and cytotoxicity were evaluated against wild type HIV-1 strain III_B and HIV-2 ROD in MT-4 cells using the 3-(4,5-dimethylthiazol-2-yl)-2,5-diphenyltetrazolium bromide (MTT) method.[12] Briefly, virus stocks were titrated in MT-4 cells and expressed as the 50% cell culture infective dose ($CCID_{50}$). MT-4 cells were suspended in culture medium at 1×10^5 cells/ml and infected with HIV at a multiplicity of infection of 0.02. Immediately after viral infection, 100 μl of the cell suspension was placed in each well of a flat-bottomed microtiter tray containing various concentrations of the test compounds. The test compounds were dissolved in DMSO at 50 mM or higher. After 4-d incubation at 37 °C, the number of viable cells was determined using the MTT method. Compounds were tested in parallel for cytotoxic effects in uninfected MT-4 cells.

3D-QSAR Model The structures were built in SYBYL 6.7 on a Silicon Graphics Octane (R10000) workstation.[19]

In our study, all the target compounds **12**—**29** were minimized using molecular mechanics with the Gasteiger–Huckel charges with a 0.005 kcal/mol energy gradient covergence criterion.

Compound **23**, the most active compound, was chosen as the template molecule on which other molecules were aligned as described by Jiang and Guo *et al.*[20,21]

The anti-HIV-1 activity of the compounds was homogeneously expressed as IC_{50} (M) and transformed to the pIC_{50} ($-\log IC_{50}$) values, which were used as the target variable in PLS regression analyses to derive 3D-QSAR models using the implementation in the SYBYL package.

The overlapped molecules were surrounded by a 3D grid of points in three dimensions extending at least 4 Å beyond the union volume occupied by the superimposed molecules. The CoMFA descriptors, steric and electrostatic field energies, were calculated using the SYBYL default parameters: 2 Å grid points spacing, an sp^3 carbon probe atom with +1 charge and a van der Waals radius of 1.52 Å, and column filtering of 2.0 kcal/mol.

General Procedure for 5-Alkyl-2,4-dimethoxy-6-(1-naphthoyl)pyrimidine 10a, b 5-Alkyl-6-chloro-2,4-dimethoxypyrimidine **8a**, **b** (100 mmol) and 1-naphthylacetonitrile (20.04 g, 120 mmol) were dissolved in anhydrous DMF (300 ml) under nitrogen atmosphere. The solution was cooled to −15 °C and NaH (4.80 g, 120 mmol) (60% in paraffin) was added portionwise. The resulting mixture was stirred for about 48 h at room temperature to give the corresponding intermediate nitriles **9a**, **b**. Then without separation, air was immediately passed through the reaction mixture at room temperature for 48—72 h. The henna solution was neutralized with acetic acid and concentrated under reduced pressure to give a red black residue **10a**, **b**, which was used without any further purification for the next step.

General Procedure for 5-Alkyl-6-(1-naphthoyl)-2,4-pyrimidinedione 11a, b To a stirred solution of **10a**, **b** (90 mmol) in methanol (450 ml), 36% HCl (225 ml) was added. The reaction mixture was refluxed for 24—48 h. A yellow precipitate, which formed, was filtered off, washed with water, and recrystallized from methanol/chloroform (5 : 1).

5-Ethyl-6-(1-naphthoyl)-2,4-pyrimidinedione (**11a**) Yield: 21.7 g (82.0%), a light yellow powder, mp: 270.9—272.0 °C. ^{1}H-NMR (DMSO-d_6) δ: 0.83 (3H, t, J=7.3 Hz), 2.03 (2H, q, J=7.2 Hz), 7.66—9.00 (7H, m), 11.20 (1H, s), 11.31 (1H, s). HR-MS m/z: 295.1086 (Calcd for $C_{17}H_{15}N_2O_3$ $[M+H]^+$: 295.1083).

5-Isopropyl-6-(1-naphthoyl)-2,4-pyrimidinedione (**11b**) Yield: 19.3 g (69.6%), a light yellow powder, mp: 228.8—231.5 °C. ^{1}H-NMR (DMSO-d_6) δ: 1.12 (6H, d, J=6.4 Hz), 2.49 (1H, sep, J=6.4 Hz), 7.69—9.22 (7H, m), 11.25 (1H, s), 11.38 (1H, s). HR-MS m/z: 309.1238 (Calcd for $C_{18}H_{17}N_2O_3$ $[M+H]^+$: 309.1239).

General Procedure for Compounds 12—29 To a solution of **11a**, **b** (2 mmol) in dry DMF (8 ml), anhydrous K_2CO_3 (2 mmol) was added. After stirring at room temperature for 0.5 h, halids (2.2 mmol) were added. The reaction mixture was stirred for additional 24—36 h. Following filtering off, the filtrate was concentrated *in vacuo* to give a brown residue, which was purified by silica column chromatography using 50% ethyl acetate/hexane (compounds **14**, **20**, **21**, **28**) and 30% ethyl acetate/hexane (other compounds) as eluents.

5-Isopropyl-1-[(2*E*,6*E*,10*E*,14*E*,18*E*,22*E*,26*E*,30*E*)-3,7,11,15,19,23,27,31,35-nonamethylhexatriaconta-2,6,10,14,18,22,26,30,34-nonaen-1-yl]-6-(1-naphthoyl)-2,4-pyrimidinedione (**24**) Yield: 1.07 g (58.3%), colorless oil. ^{1}H-NMR ($CDCl_3$) δ: 1.17 (6H, d, J=6.9 Hz), 1.55 (9H, s), 1.60 (21H, s), 1.98—2.08 (32H, m), 2.44 (1H, sep, J=6.9 Hz), 4.29 (2H, s), 4.95—5.13 (9H, m), 7.54—8.18 (7H, m), 9.39 (1H, s). HR-MS (MALDI): 943.6682 (Calcd for $C_{63}H_{88}N_2NaO_3$ $[M+Na]^+$: 943.6693).

1,3-Di[(2*E*)-3-phenylallyl]-5-isopropyl-6-(1-naphthoyl)-2,4-pyrimidinedione **(29)** Yield: 0.39 g (36.1%), a yellow powder, ^{1}H-NMR ($CDCl_3$) δ: 1.19 (6H, d, J=6.9 Hz), 2.52 (1H, sep, J=6.9 Hz), 4.40—4.43 (2H, m), 4.77—4.79 (2H, m), 6.04—6.05 (2H, m), 6.38—6.41 (1H, m), 6.79 (1H, m), 7.01—7.33 (10H, m), 7.43—8.10 (7H, m). HR-MS (MALDI): 563.2309 (Calcd for $C_{36}H_{32}N_2NaO_3$ $[M+Na]^+$: 563.2311).

References and Notes

1) For Part 6, see: Sun G. F., Kuang Y. Y., Chen F. E., Wang Y. P., De Clercq E., Balzarini J., Pannecouque C., *Arch. Pharm. Chem. Life Sci.*, **338**, 1—5 (2005).
2) De Clercq E., *Antiviral Res.*, **38**, 153—179 (1998).
3) Baba M., Tanaka H., De Clercq E., Pauwels R., Balzarini J., Schols D., Nakashima H., Perno C. F., Walker R. T., Miyasaka T., *Biochem. Biophys. Res. Commun.*, **165**, 1375—1381 (1989).
4) Miyasaka T., Tanaka H., Baba M., Hayakawa H., Walker R. T., Balzarini J., De Clercq E., *J. Med. Chem.*, **32**, 2507—2509 (1989).
5) Danel K., Larsen E., Pedersen E. B., *Synthesis*, **8**, 934—936 (1995).
6) Tanaka H., Baba M., Hayakawa H., Sakamaki T., Miyasaka T., Ubasawa M., Takashima H., Sekiya K., Nitta I., Shigeta S., Walker R. T., Balzarini J., De Clercq E., *J. Med. Chem.*, **34**, 349—351 (1991).
7) Meng G., Chen F. E., De Clercq E., Balzarini J., Pannecouque C., *Chem. Pharm. Bull.*, **51**, 779—789 (2003).
8) Sun G. F., Chen X. X., Chen F. E., Wang Y. P., De Clercq E., Balzarini J., Pannecouque C., *Chem. Pharm. Bull.*, **53**, 886—892 (2005).
9) Hopkins A. L., Ren J., Esnouf R. M., Willcox B. E., Jones E. Y., Ross C., Miyasaka T., Walker R. T., Tanka H., Stammers D. K., Stuart D. I., *J. Med. Chem.*, **39**, 1589—1600 (1996).
10) Baddiley J., Topham A., *J. Chem. Soc.*, **1944**, 678—679 (1944).
11) Merkatz A. V., *Ber. Dtsch. Chem. Ges.*, **52**, 869—880 (1919).
12) Pauwels R., Balzarini J., Baba M., Snoeck R., De Clercq E., *J. Virol. Methods*, **20**, 309—322 (1988).
13) Ragno R., Mai A., Sbardella G., Artico M., Massa S., Cadeddu A., Colla P., *J. Med. Chem.*, **47**, 928—934 (2004).
14) Hannongbua S., Lawtrakul L., *Quant. Struct.-Act. Relat.*, **15**, 389—394 (1996).
15) Alves C. N., Pinheiro J. C., Camargo A. J., Ferreira M. M. C., Da Silva A. B. F., *J. Mol. Struct.* (*Theochem.*), **530**, 39—47 (2000).
16) Wold S., Rhue A., Wold H., Dunn W. J. I., *SAIM J. Sci. Stat. Comput.*, **5**, 735—743 (1994).
17) Wold S., Albano C., Dunn W. J., III, Edlund U., Esbensen K., Geladi P., Hellberg S., Johanson E., Lindberg W., Sjostrom M., *NATO ASI Ser., Ser. C*, **138**, 17—95 (1984).
18) Clark M., Cramer I. R. D., *Quant. Struct.-Act. Relat.*, **12**, 137—145 (1993).
19) Sybyl, version 6.7; Tripos Associates; St. Louis, MO, Tripos, Inc., 2000.
20) Hong L., Huang X. Q., Shen J. H., Luo X. M., Li M. H., Xiong B., Chen G., Shen J. K., Yang Y. M., Jiang H. L., Chen K. X., *J. Med. Chem.*, **45**, 4816—4827 (2002).
21) Guo Y. S., Xiao J. F., Guo Z. R., Chu F. M., Cheng Y. H., Wu S., *Bioorg. Med. Chem.*, **13**, 5424—5434 (2005).